ACS OMEGA

http://pubs.acs.org/journal/acsodf

Article

A Novel Distributed Fault Detection Approach Based on the Variational Autoencoder Model

Chenghong Huang, Yi Chai,* Zheren Zhu, Bowen Liu, and Qiu Tang

Cite This: *ACS Omega* 2022, 7, 2996−3006

Read Online

ACCESS | Metrics & More | Article Recommendations

ABSTRACT: In large-scale industrial fault detection, a distributed model is typically established on the basis of blocked units. However, blocked distributed methods consider units as independent of one another and disregard the relationship between units, thus leading to incomplete information on local units. In fact, the operation status of a unit is affected by a local unit and its surrounding neighboring units. In addition, the fault detection performance of a system is seriously reduced once data are missing from the data source. Variational autoencoder (VAE) is not only a popular deep generative model but also has a powerful nonlinear feature extraction capability. In this study, VAE is extended to the distributed case. In this study, a distributed fault detection method DVAE based on VAE is proposed. This method can not only describe local and neighboring information, but it can also reconstruct missing data. First, system variables are divided into local and neighboring units in accordance with the system mechanism. Second, for each local unit, a DVAE model is established to map the multivariable data onto the latent variable space. The obtained latent variable contains the information on a local unit and can reflect the complex relationship with its neighboring units. Lastly, Euclidean distance is used to detect system faults. When applied on the Tennessee Eastman process for verification, the proposed method shows good performance in fault detection and missing data reconstruction.

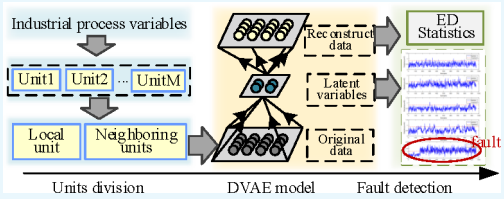

INTRODUCTION

With the continuous improvement of operation safety and product quality requirements, fault detection technology for industrial processes has attracted increasing attention.[1−3] In the initial stage, model-based approaches are the mainstream by analyzing the residuals of actual and estimated values. However, owing to the continuous scale, complexity, and integration of complex industrial processes, process data are characterized by redundancy, high dimension, and nonlinearity. An accurate mechanism model of the system is increasingly difficult to obtain, thereby posing a new challenge to traditional fault diagnosis methods. Owing to the development of computer and sensor technology, extensive data reflecting the operation state of the system can be collected and saved, and the fault detection method driven by data has developed rapidly. This type of method does not need an accurate mechanism model and does not rely on empirical knowledge, thereby leading to the popularity of this research field.[4,5]

Multivariate statistics approaches, which are some of the data-driven methods used for industrial process fault detection, project the monitored multivariable sample space onto a low-dimensional subspace that is composed of latent variables. These methods first reduce the dimension of the high-dimensional observation data and construct monitoring statistics in the low-dimensional space to realize fault detection. They are a major component of current studies[6] and typically include principal component analysis (PCA),[7] linear discriminant analysis,[8] locality-preserving projections,[9] independent component analysis,[10] and their extensions.[11,12] Considerable nonlinearity constantly exists in process data because of the complex physical and chemical reaction characteristics between variables. Kernel methods (e.g., kernel PCA[13] and kernel Fisher linear discrimination[14]) have received widespread attention. Despite the widespread use of kernel approaches, kernel determination remains a considerable challenge.[15] Due to the immense power in extracting the intrinsic feature, machine learning methods have received more and more attention. Such methods include self-organizing maps,[16] deep belief networks,[17] Gaussian belief networks,[18] Bayesian network,[19,20] and autoencoder (AE).[21,22] Among these methods, AE is an efficient and flexible unsupervised learning dimensionality reduction model for large-scale data. It plays a central role because of its excellent performance in data reconstruction. Variational AE (VAE),[23] an extension of AE, can find an efficient latent variable space as a multivariate normal distribution by adding a constraint on the coding network and can be regarded as the nonlinear form of

Received: October 28, 2021
Accepted: December 24, 2021
Published: January 11, 2022

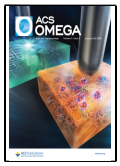

https://doi.org/10.1021/acsomega.1c06033
ACS Omega 2022, 7, 2996−3006

probabilistic PCA. VAE applies variational Bayesian inference in parameter estimation and introduces AE into the generative framework. It can be used for dimensionality reduction, reconstruction, and generation and has thus attracted extensive attention in recent studies.

With the expansion of the production scale and the progress of instrument monitoring technology, processes have become characterized by large scales, multiple operating units, and complex interactions.[24,25] The failure of a unit affects the entire production process. A global monitoring model is easily affected by irrelevant information. Therefore, numerous distributed methods have been proposed to address large-scale plant-wide processes. In distributed fault detection, the whole process is divided into sub-blocks in accordance with process knowledge or data characteristic analysis.[26] For example, He[27] proposed an online distributed process monitoring and alarm analysis system by using novel canonical variate analysis with multicorrelation blocks. In consideration of the difficulty encountered in dividing process variables without any prior knowledge, Xu[28] proposed a block division strategy that is based on maximal information coefficient−spectral clustering. This strategy can divide the process variables into several blocks without any prior knowledge. However, these methods only consider the local block and disregard relationships with their surroundings. In consideration of the inherent connection between blocks, Cao[29] developed a distributed PCA method that is based on the industrial process connection. Jiang[30] proposed a variational Bayesian-based PCA method for distributed process monitoring. Jiang[31] proposed a local−global modeling and distributed computing framework for handling complex nonlinear processes. Although these works have enhanced the performance of industrial fault detection, they do not incorporate variable relationships with surrounding neighboring units into the generative framework and show weak robustness when data are missing. In fact, the problems of large scale, nonlinearity, and missing samples often coexist simultaneously in practical production. Consequently, a distributed nonlinear detection method that reflects the complex relationship with neighboring units and then reconstructs missing data is necessary.

This study aims to propose a distributed probabilistic model based on VAE, namely, DVAE, which incorporates deep VAE and the blocked distributed computing technique. First, the proposed DVAE model divides system variables into local and neighboring units in accordance with the system mechanism. Second, for each local unit and its corresponding neighboring units, a DVAE probability model that takes into account the local and neighboring information is constructed to map the complex distributed process data onto the latent variable space. Third, monitoring statistics based on Euclidean distance (ED) are calculated based on calculated latent variables, which realize the fault detection and fault location of local faults. Given that process data usually violate the Gaussian distribution assumption, the confidence limits of the DVAE in each block are determined by kernel density estimation (KDE). The main contributions of this paper are as follows.

(1) VAE is not only a popular deep generative model, but it also has a powerful nonlinear feature extraction capability. However, the application of VAE in industrial fault detection is insufficient. This study extends VAE to distributed fault detection in industrial processes. In principle, this improvement may also be used in other generative models.
(2) The proposed method is a distributed fault detection method for industrial processes. It can describe the correlation between local unit data and latent variables as well as reflect complex relationships with neighboring units.
(3) The proposed method has strong data reconstruction capability. In the case study, we use reconstructed data to replace randomly missing data, and the proposed method exhibits good performance in missing data processing.

The remainder of the paper is organized as follows. Section 2 introduces the basic theory of VAE. Section 3 presents the proposed model DVAE and discusses the framework of fault detection based on DVAE. Section 4 applies the proposed model to verify the performance of fault detection. Lastly, Section 5 provides the conclusions.

PRELIMINARIES

VAE is a popular generative model for nonlinear dimension reduction, which combines Bayesian inference with deep neural networks.[23] As shown in Figure 1, the structure of VAE comprises two parts: encoder and decoder. Observed data $\mathbf{x} = [x_1, x_2, ..., x_n]^T$ are generated by some random process and involve the latent variables $\mathbf{z} = [z_1, z_2, ..., z_k]^T$, and $\mathbf{x}$ can be reconstructed by $\mathbf{z}$ through a generation model. The recognition model $q_\phi(z|x)$ is considered a probabilistic encoder, and $p_\theta(x|z)$ is considered a probabilistic decoder.

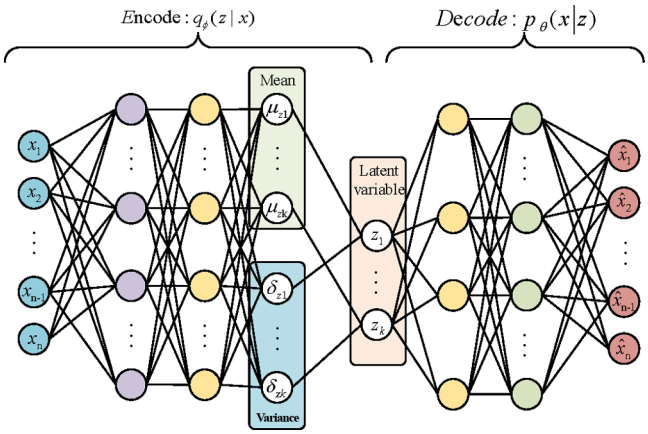

Figure 1. Illustration of the VAE structure.

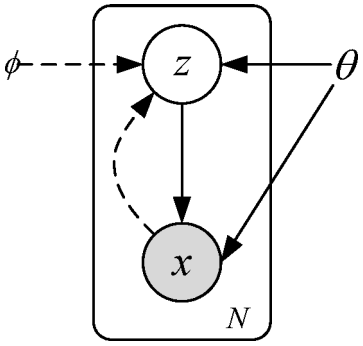

Figure 2. Illustration of the VAE architecture.

https://doi.org/10.1021/acsomega.1c06033
ACS Omega 2022, 7, 2996−3006

Figure 2 shows the graphical representation of VAE. The shaded and hollow circles represent observed and latent variables, respectively. Arrows imply dependencies, and plates indicate the number of instances.

VAE approximates the distribution of latent variables to a multivariate normal distribution $p(z^{(i)}) = \mathcal{N}(0, \mathbf{I})$. The recognition model $q_\phi(z|x)$ is described as a multivariate normal distribution. That is, for a given data point $\mathbf{x}$, the encoder derives the mean vector $\boldsymbol{\mu}_z = [\mu_{z_1}, \mu_{z_2}, ..., \mu_{z_k}]^T$ and variance vector $\boldsymbol{\delta}_z^2 = [\delta_{z_1}^2, \delta_{z_2}^2, ..., \delta_{z_k}^2]^T$. For this reason, dimensionality reduction based on VAE is feasible.

The assumption is that the observed samples are independent, and the goal of VAE is to estimate the unknown parameters and latent variables by maximizing the log-likelihood function as follows:

$$\log p(x) = \sum_{i=1}^{N} \log p(x^{(i)}) \tag{1}$$

In variational inference, the marginal likelihood of each individual data point is written as follows

$$\log p_\theta(x^{(i)}) = \mathrm{KL}(q_\phi(z|x^{(i)}) \| p_\theta(z|x^{(i)})) + \mathcal{L}(\theta, \phi; x^{(i)}) \tag{2}$$

where ϕ are the variational parameters, θ are the generative parameters, $p_\theta(x^{(i)})$ are the marginal likelihood of the ith data points, KL( ) is the KL divergence of the approximate $q_\phi(z|x^{(i)})$ from the true posterior $p_\theta(z|x^{(i)})$, and $\mathcal{L}(\theta, \phi; x^{(i)})$ is called the variational lower bound on the marginal likelihood of the ith data points, which is written as follows:

$$\begin{aligned}
\mathcal{L}(\boldsymbol{\theta}, \phi; x^{(i)}) &= \mathbb{E}_{q_\phi(z|x)}[-\log q_\phi(z|x^{(i)}) + \log p_\theta(x^{(i)}, z)] \\
&= \mathbb{E}_{q_\phi(z|x)}[-\log q_\phi(z|x^{(i)}) + \log p_\theta(x^{(i)}|z) p_\theta(z)] \\
&= \mathbb{E}_{q_\phi(z|x)}\left[\frac{-\log q_\phi(z|x^{(i)})}{p_\theta(z)} + \log p_\theta(x^{(i)}|z)\right] \\
&= -\mathrm{KL}(q_\phi(z|x^{(i)}) \| p_\theta(z)) + \mathbb{E}_{q_\phi(z|x^{(i)})}[\log p_\theta(x^{(i)}|z)]
\end{aligned} \tag{3}$$

Given that the KL divergence is non-negative, we obtain $\log p_\theta(x^{(i)}) \geq \mathcal{L}(\theta, \phi; x^{(i)})$. The maximize marginal likelihood problem is converted into maximizing the lower bound $\mathcal{L}(\theta, \phi; x^{(i)})$. Thereafter, the loss function is a minimized eq 4

$$\mathrm{KL}(q_\phi(z|x^{(i)}) \| p_\theta(z)) - \mathbb{E}_{q_\phi(z|x^{(i)})}[\log p_\theta(x^{(i)}|z)] \tag{4}$$

where the first term is the regularized constraint item to make the approximate posterior as close to the prior distribution as possible. The second term represents the expectation of negative reconstruction error, which can force the output as close to the input as possible.

In general, the term of KL divergence can obtain an accurate analytic solution. However, obtaining the analytic solution for calculating the expectation $\mathbb{E}_{q_\phi(z|x^{(i)})}[\log p_\theta(x^{(i)}|z)]$ of eq 4 is difficult because of the integral. The reparameterization strategy is used to estimate the true expectation with the samplings. For $\mathbf{z}^{(i)} = [z_1^{(i)}, z_2^{(i)}, ..., z_l^{(i)}]^T$, which is sampled from $p_\theta(z|x^{(i)})$, the expectation is calculated as follows

$$\mathbb{E}_{q_\phi(z|x^{(i)})}[\log p_\theta(x^{(i)}|z)] \approx \frac{1}{L}\sum_{i=1}^{L} \log p_\theta(x^{(i)}|z) \tag{5}$$

where $z = \mu^{(i)} + \sigma^{2(i)} \times \varepsilon^{(l)}$, $\varepsilon^{(l)} \sim \mathcal{N}(0, 1)$, and L is the number of sampling.

PROPOSED METHODOLOGY

Proposed DVAE Model. The entire process is divided into multiple subsets $U = [U_1, U_2, ..., U_n]$ according to the mechanism knowledge. Observed data of the local unit U_i are denoted as $\mathbf{x} = [x_1, x_2, ..., x_p]^T$, and the neighboring units $U_{j\neq i}$ are denoted as $\mathbf{y} = [y_1, y_2, ..., y_q]^T$. Moreover, $\mathbf{t} \in \mathfrak{R}^{D\times n}$ is used to stand for all of the related data: $\mathbf{t} = [\mathbf{x}^T, \mathbf{y}^T]^T$. Given that the latent variables of the local unit are related with U_i and also with its neighboring units $U_{j\neq i}$, the model of distributed fault detection can be described as follows

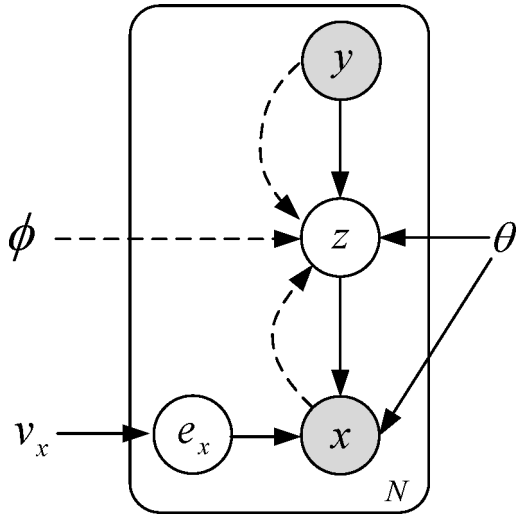

Figure 3. Illustration of the VAE architecture.

$$\begin{aligned}
z &= f(t) + e_x \\
x &= g(z) + e_x
\end{aligned} \tag{6}$$

where $z \in \mathfrak{R}^{k\times n}$ is the latent variable and $p(z) \sim N(0, I)$, k is the dimension of latent space, n is the data number, $e_x \in \mathfrak{R}^{D\times n}$ is the noise, $p(e_x) \sim N(0, v_x I)$, v_x is the variance, $p(v_x) \sim \mathrm{IGamma}(a_0, b_0)$, and D is the dimension of the observed data. The Gaussian model is used to approximate the distribution of z, and the encode process is expressed as $p(z|t) \sim N(\mu(t), \delta^2(t))$, $p(v_x|t) \sim \mathrm{Halfnormal}(\theta)$. The Gaussian model is used to generate the original data, and the decode process is expressed as $p(x|z, v_x) \sim N(f(z), v_x I)$.

The graphical representation of the proposed model is shown in Figure 3. Note that the latent variable z is influenced by the local unit and its neighboring units.

Approximate Inference. The objective is to estimate the posterior probabilities of latent variable z, given the observed data. Once z is obtained, dimensionality reduction is achievable. Faults may be detected using some statistical indexes. Given that direct inference is analytically intractable, an approximated distribution $q_\phi(z|x^{(i)})$ is used, similar to VAE. Model evidence $\log p_\theta(X)$ can be decomposed as

https://doi.org/10.1021/acsomega.1c06033
ACS Omega 2022, 7, 2996−3006

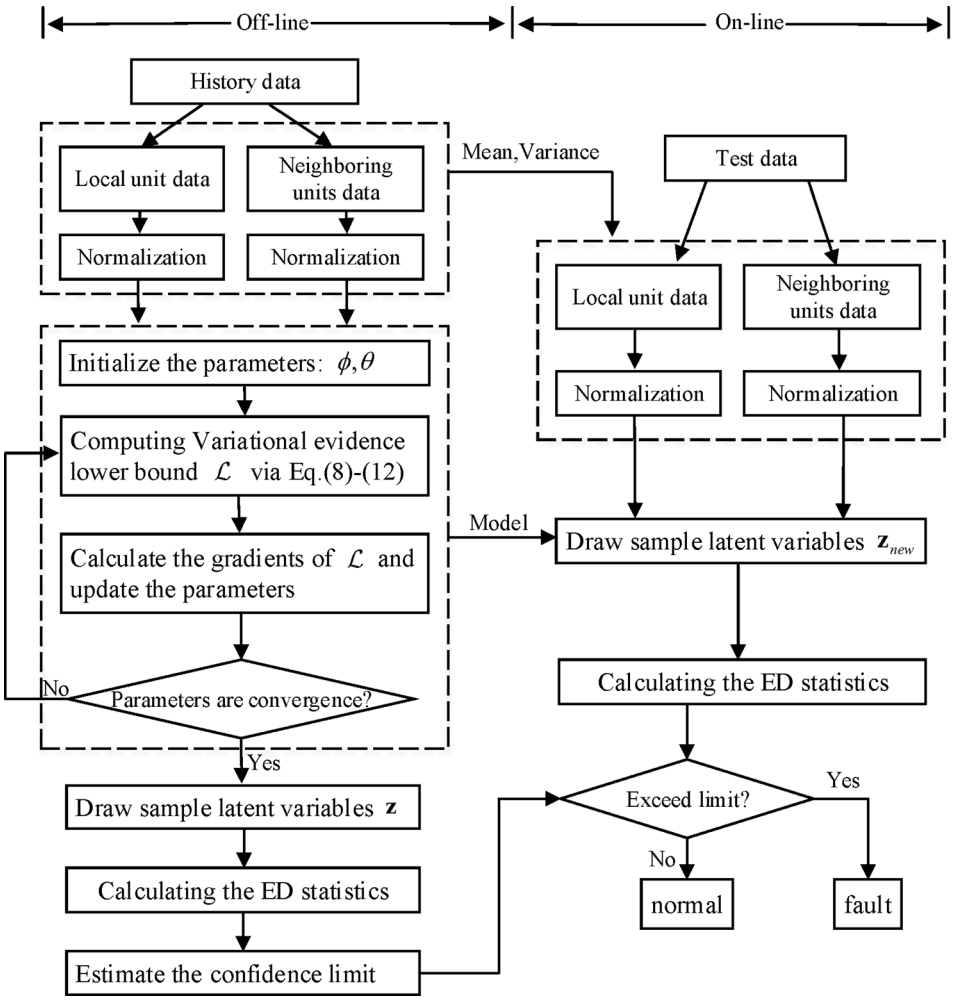

Figure 4. Fault detection procedure of the proposed DVAE model.

$\sum_{i=1}^{N} \log p_\theta(x_i)$. Variational posterior $q_\phi(z, v_x|t)$ can be decomposed as $q_\phi(v_x) \prod_{i=1}^{N} (z_i|t_i)$ and

$$\log p(x_i) \geq \mathcal{L}(x_i, \phi, \theta) = \mathbb{E}_{q_\phi(z_i, v_x|t_i)}[\log p(x_i, z_i, v_x) - q_\phi(z_i, v_x|t_i)] \tag{7}$$

which can be derived as follows

$$\mathcal{L}(x_i, \phi, \theta) = \underbrace{-\mathrm{KL}(q_\phi(z_i|t_i)\|p(z_i))}_{1} - \underbrace{\mathrm{KL}(q_\phi(v_x)\|p(v_x))}_{2} + \underbrace{\mathbb{E}_{q_\phi(z_i, v_x|t_i)}[\log p(x_i|z_i, v_x)]}_{3} \tag{8}$$

The first term of eq 8 has an accurate analytic solution as follows:

$$-\mathrm{KL}(q_\phi(z_i|t_i)\|p(z_i)) = \frac{1}{2}\sum_{j=1}^{J}(1 + \log[\delta_j^{(i)}(t_i)]^2 - [\mu_j^{(i)}]^2 - [\sigma_j^{(i)}(t_i)]^2) \tag{9}$$

Monte Carlo sampling estimation is used to estimate the other two terms. z_i and v_x are sampled by

$$z_i \sim N(\mu^{(i)}(t_i), \delta^{2^{(i)}}(t_i))$$
$$v_x \sim \text{Half Normal}(\theta) \tag{10}$$

The reparameterization strategy is also applied in our model to obtain a differentiable estimator

$$-\mathrm{KL}(q_\phi(v_x)\|p(v_x)) + \mathbb{E}_{q_\phi(z_i, v_x|t_i)}[\log p(x_i|z_i, v_x)] \approx \frac{1}{L}\sum_{i=1}^{L}[\log p(z_i^{(l)}) - \log q(v_x^{(l)}) + \log p(x_i|z_i^{(l)}, v_x^{(l)})] \tag{11}$$

where

$$z_i^{(l)} = (\mu^{(i)}(t_i) + \delta^{2^{(i)}}(t_i)\cdot\varepsilon_i^{(l)}, \text{ and } \varepsilon_i^{(l)} \sim \mathcal{N}(0, 1)$$
$$v_x^{(l)} = \sqrt{\theta}\cdot|\delta^{(l)}|, \text{ and } \delta^{(l)} \sim \mathcal{N}(0, 1) \tag{12}$$

Fault Detection. Given the local unit $\mathbf{x} = [x_1, x_2, ..., x_p]^T$ and with the neighboring units training data set $\mathbf{y} = [y_1, y_2, ..., y_q]^T$ representing the training data set, the latent variable $\mathbf{z} = [z_1, z_2, ..., z_k]^T$ is obtained through the DVAE model. The Euclidean metric is the distance representation of two points in the Euclidean space, which is the simplest and most widely used to reflect the similarity between two signals. On this basis, the monitoring quantity based on ED is established as follows:

https://doi.org/10.1021/acsomega.1c06033
ACS Omega 2022, 7, 2996−3006

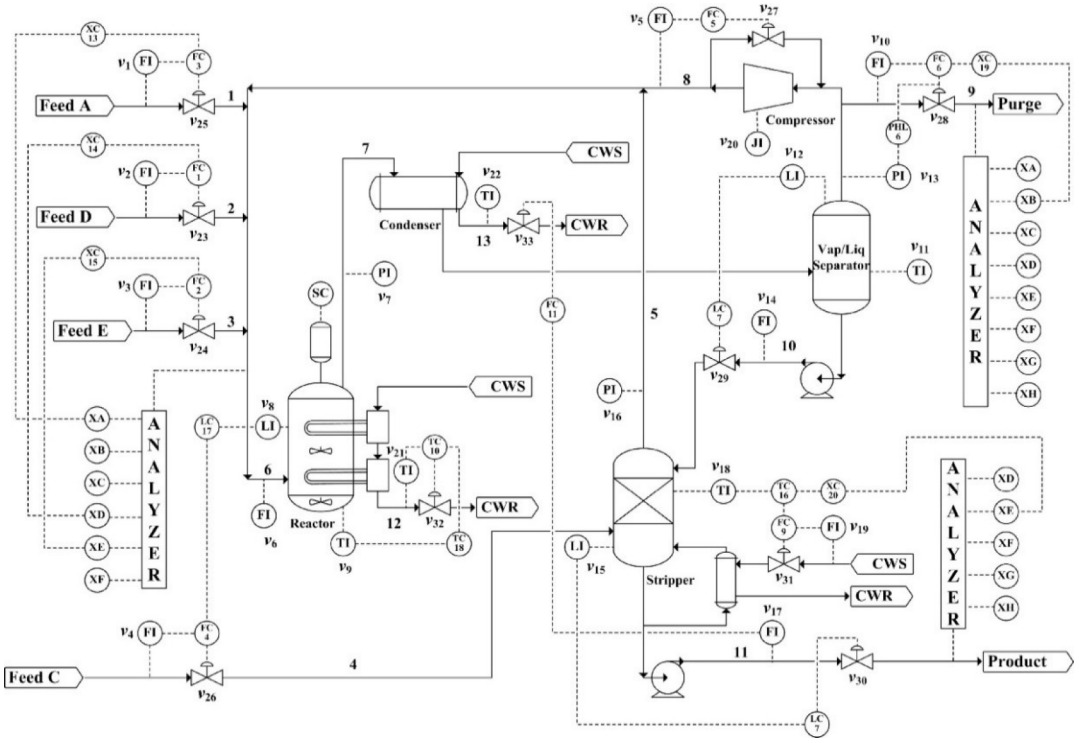

Figure 5. Tennessee Eastman process flowchart.

$$\mathbf{D}(\boldsymbol{x}, \boldsymbol{y}) = \sqrt{(x_1 - y_1)^2 + (x_2 - y_2)^2 + \ldots + (x_n - y_n)^2} = \sqrt{\sum_{i=1}^{n} (x_i - y_i)^2} \tag{13}$$

Suppose the confidence limit of $\bar{\mathbf{D}}$ exists; whether the statistical distribution of $\mathbf{D}$ is normal or abnormal is to judge whether they have exceeded the control limit. This study considers that the actual process data distribution is unknown and there is noise and error interference. Hence, KDE is used to calculate the confidence limit. The statistics of training samples is denoted as the same variable $\mathbf{S}^2 = [s_1^2, s_2^2, \ldots, s_n^2]$, and the probability distribution density of $\mathbf{S}^2$ is estimated using KDE as follows

$$\hat{f}(\mathbf{S}^2) = \frac{1}{n\gamma} \sum_{i=1}^{n} k\left(\frac{s^2 - s_i^2}{\gamma}\right) \tag{14}$$

where n is the number of training samples, γ is the window width (smoothing parameter), and $k(\cdot)$ is the kernel function. This research selects the Gaussian kernel function, and the probability distribution density can be described as follows:

$$\hat{f}(\mathbf{S}^2) = \frac{1}{n\gamma\sqrt{2\pi}} \sum_{i=1}^{n} \exp\left(-\frac{(s^2 - s_i^2)}{2\gamma^2}\right) \tag{15}$$

Given the confidence limit of normal samples, process faults will be detected if the statistics of new samples exceeds the confidence limit.

Detection Procedure. The entire detection procedure of the fault detection based on DVAE is shown in Figure 4.

I: Off-line training process:

1. Acquire normalized local unit data $\mathbf{x} = [x_1, x_2, \ldots, x_p]^T$ and neighboring unit data $\mathbf{y} = [y_1, y_2, \ldots, y_q]^T$ as training samples under the normal running state.
2. Initialize the parameters ϕ and θ.
3. Compute the variational evidence lower bound $\mathcal{L}$ by using eqs 8−12.
4. Calculate the gradients of $\mathcal{L}$ and update the parameters.
5. Determine whether ϕ and θ are converged. If not, return to step 3.
6. Draw sample latent variables $\mathbf{z} = [z_1, z_2, \ldots, z_l]^T$ through the trained DVAE model.
7. Construct a fault detection model by calculating the ED statistics of training data.
8. Estimate the confidence limit based on the KDE model.

II: Online detection process:

1. Acquire the new local unit data $\mathbf{x}_{new}$ and the new neighboring units data $\mathbf{y}_{new}$ and normalize them with the mean and variance of training samples.
2. Draw sample latent variables $\mathbf{z}_{new} = [z_{1new}, z_{2new}, \ldots, z_{lnew}]^T$ of test data through the trained DVAE model.
3. Calculate the ED statistics of the test data.
4. Monitor whether the ED statistics exceeds the confidence limit obtained in step 6 in the offline process.
5. Calculate the fault detection rate (FDR).

CASE STUDY

Tennessee Eastman Process. The Tennessee Eastman (TE) process is a simulated benchmark platform developed by Downs and Vogel based on a realistic chemical industrial process. The system simulation can be found from http://web.mit.edu/braatzgroup/links.html. This process is widely used to verify the fault detection performance in industrial process fault detection. The TE process consists of five main operating units: continuous stirring-type reactor, condenser, recycling compressor, vapor−liquid separator, and stripping tower (see Figure 5[32]). This process is also comprised of 52 variables: 12 manipulated variables, 19 composition measurements, and 22

https://doi.org/10.1021/acsomega.1c06033
ACS Omega 2022, 7, 2996−3006

Table 1. Operating Units and Corresponding Variables in the TE Process

variable description	variable name	unit
A feed (flow 1)	XMEAS1	feed
D feed (flow 2)	XMEAS2	
E feed (flow 3)	XMEAS3	
A & C feed	XMEAS4	
D feed flow	XMV1	
A feed flow	XMV2	
E feed flow	XMV3	
A & C feed flow	XMV4	
reactor feed flow	XMEAS6	reactor
reactor pressure	XMEAS7	
reactor liquid level	XMEAS8	
reactor temperature	XMEAS9	
reactor water temperature	XMEAS21	
reactor cooling water feed flow	XMV10	
condenser cooling water feed flow	XMV11	
separator temperature	XMEAS11	separator
separator liquid level	XMEAS12	
separator pressure	XMEAS13	
separator bottom flow	XMEAS14	
separator water temperature	XMEAS22	
separator liquid flow	XMV7	
stripper liquid level	XMEAS15	stripper
stripper pressure	XMEAS16	
stripper bottom flow	XMEAS11	
stripper temperature	XMEAS11	
stripper steam flow	XMEAS11	
stripper produce flow	XMV8	
stripper steam valve opening	XMV9	
recirculation flow	XMEAS5	compress
discharge rate	XMEAS10	
compressor power	XMEAS21	
compressor recirculation valve	XMV5	
drain valve	XMV6	

Table 2. Disturbances in the Tennessee Eastman Process

number	disturb	type
1	A/D feed ratio changes, B composition constant	step
2	B feed ratio changes, A/D composition constant	step
3	D feed temperature changes	step
4	reactor cooling water inlet temperature changes	step
5	condenser cooling water inlet temperature changes	step
6	A feed loss	step
7	C head pressure loss	step
8	A/B/C composition changes	random
9	D feed temperature changes	random
10	C feed temperature changes	random
11	reactor cooling water inlet temperature changes	random
12	separator cooling water inlet temperature changes	slow drift
13	reactor dynamic constant changes	slow drift
14	reactor valve	sticking
15	separator valve	sticking
16	unknown	unknown
17	unknown	unknown
18	unknown	unknown
19	unknown	unknown
20	unknown	unknown
21	stable valve in stream 4	constant

Table 3. Average FDR (%) with Different Network Layers

encode/decode	2	3	4	5
2	50.33	47.96	42.28	42.32
3	45.11	47.16	43.18	42.66
4	51.56	52.11	40.37	41.35
5	52.60	43.12	43.18	43.87
6	44.8	43.53	42.87	43.79

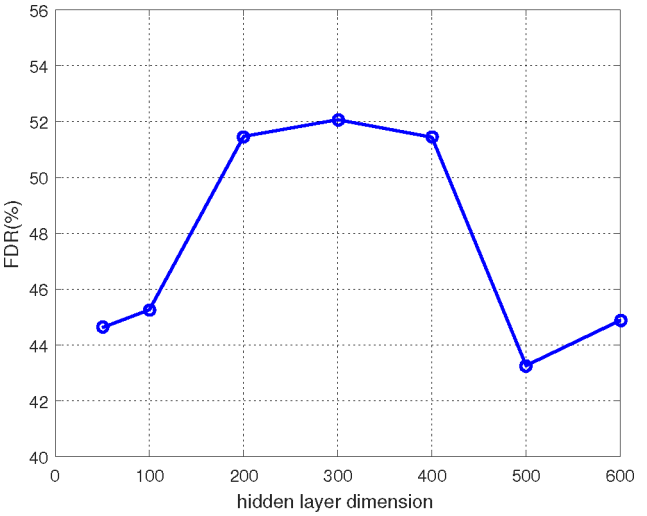

Figure 6. Average FDR with different hidden layer dimension.

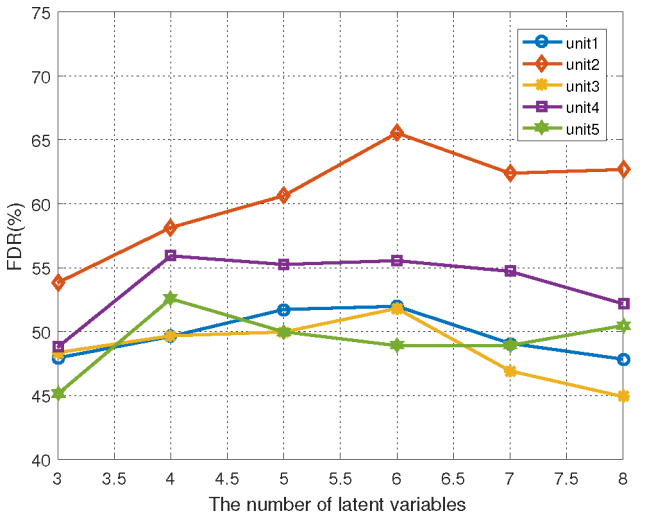

Figure 7. Average FDR with different hidden layer dimension.

continuous variables. In this study, 22 continuous and 12 manipulated variables under normal states are selected as the training data set, and 21 types of fault data are chosen as the test data set. Corresponding variables and units are listed in Table 1.[30,32,33] The five units from top to bottom are called units 1−5.

Table 2 shows that TE data consist of 21 types of fault and normal data: faults 1−7 are step faults; faults 8−12 are caused by random changes in variables; fault 13 is a variable slow drift fault; faults 14, 15, and 21 are caused by valve sticking; and faults 16−20 are unknown faults. Each data set includes 960 samples. In the fault state, all types of faults are injected at the 161st sample.

https://doi.org/10.1021/acsomega.1c06033
ACS Omega 2022, 7, 2996−3006

Table 4. FDR (%) of Five Units in the TE Process

fault/unit	unit 1	unit 2	unit 3	unit 4	unit 5	DVAE
fault 1	99.12	39.3	34.29	93.62	51.06	99.12
fault 2	96.5	89.49	95.12	97.5	98.62	98.62
fault 4	4.88	100	6.76	10.64	3.75	100
fault 5	25.41	26.53	19.52	31.04	27.41	31.04
fault 6	98.75	99.75	98.87	98.37	99.62	99.75
fault 7	100	37.67	33.17	49.44	43.80	100
fault 8	89.36	90.24	90.86	92.62	96.37	96.37
fault 10	24.66	27.03	22.78	52.32	34.54	52.32
fault 11	6.38	90.71	7.63	22.78	4.63	90.71
fault 12	86.36	93.87	97.87	93.49	87.86	97.87
fault 13	85.86	88.61	86.36	93.87	84.23	93.87
fault 14	15.02	100	1.63	6.76	3.13	100
fault 16	14.14	17.4	13.39	49.69	23.28	49.69
fault 17	46.18	96.12	29.66	36.67	30.79	96.12
fault 18	89.49	88.36	90.24	87.86	88.99	90.24
fault 19	4.38	11.51	2.88	11.26	80.48	80.48
fault 20	12.77	14.27	44.56	37.05	70.59	70.59
fault 21	6.26	46.43	30.41	59.95	13.14	59.95

Parameter Selection and Model Training. To study the impact of neural network depth, the number of recognition and generation models are tested. Given that the amount of data is not considerably large, the range of depth is set from 2 to 6. Note that detecting faults 3, 9, and 15 is extremely difficult for all methods because there are not any observable changes in the means, variance, or peak time. They have minimal effects on the measured variables because they are weak faults.[34−36] Thus, the three failures are not considered in our study and the average FDR (the number of faults detected correctly/the number of faults) mentioned below does not include faults 3, 9, and 15. In addition, the false alarming rate (FAR: the number of normal samples that are detected as faults/the number of normal samples) is always associated with the FDR, and the FAR of nonlinear methods is slightly higher than that of linear methods. Thus, we restrict the FAR in an appropriate range (<2%) to filter the results. If unit 5 is used as an example, then the average FDR with variable network depth is shown in Table 3. The average FDR is naturally not satisfactory because a single unit is insensitive to some faults. However, all units have a similar change tendency with the variation of parameters and it is reasonable to tune parameters with a single unit. Overall, FDR decreases with increasing depth of the generation model, and the recognition model depth reached its maximum at 5.

We set the recognition and generation models' depth at 2 and 5, respectively, and change the dimension of the hidden layer. As shown in Figure 6, when the dimension is below 300, FDR increases with increasing hidden layer dimension. Above 300, FDR decreases or shows minimum change with increasing hidden layer dimension. The primary reason is that the size of the network parameters increases with the increase in layer sizes; the proposed approach may suffer from an overfitting problem and tends to degrade detection performance under limited training samples. Thus, the proper number of hidden layer dimension in this study is 300. In addition, the leaky ReLU is used as an activation function for the hidden layers of the encoder and decoder because it enables the efficient training of deep neural networks.[37,38]

Note that, except for the network structure, the latent variable number significantly impacts the performance of the proposed approach. The reason is that insufficient quantity leads to lack of information. By contrast, considerably large latent variables will lead to information redundancy, such as the noise information. Hence, we also turned the number of latent variable of 5 units with fixed neural network parameters. In particular, the average FDR over different latent variables is shown in Figure 7. The result shows that the units obtain the highest detection rate when the number of latent variables is 5, 6, 6, 4, and 4.

Fault Detection Results. The five units have been verified to evaluate the detection performance of the proposed method, and the maximum FDR of the five units is considered to be the detection results of DVAE. As shown in Table 4, the FDRs of

Table 5. FDR (%) of DVAE and Comparative Methods in the TE Process

	KPCA		GLPP		SPCA[39]		NDPCA[15]					
fault	T2	SPE	T2	SPE	T2	SPE	T2	SPE	DBN[12]	VAE	DPCA	DVAE
fault 1	99.75	99.38	99.25	99.37	99.86	99.36	99.5	99.5	98	99.87	99.5	99.12
fault 2	98.25	98.13	98.62	98.25	99.55	96.69	98.12	98.5	97	98.50	98.13	98.62
fault 4	81.13	93.15	3.75	57.32	13.21	10.81	13.77	12.28	97	90.49	99.75	100
fault 5	23.5	23.38	99.37	24.41	12.76	10.29	35.71	38.47	70	25.66	21.63	31.04
fault 6	99.63	99.5	100	100	100	100	100	100	99	99.50	99.75	99.75
fault 7	100	100	100	100	20.27	18.81	49.69	53.57	100	100	99.75	100
fault 8	97.25	97.5	96.50	97.62	98.07	97.81	97.75	98.25	72	97.75	96.75	96.37
fault 10	30.88	38.88	35.17	38.67	70.9	46.26	56.8	58.32	47	41.30	32.38	52.32
fault 11	62.25	61.25	19.52	53.94	86.31	90.43	23.78	29.66	68	64.83	86.75	90.71
fault 12	98.5	98.38	98.5	98.5	51.19	43.52	97.37	97.87	77	98.75	97.38	97.87
fault 13	94.75	94.25	94.12	94.37	96.1	94.33	94.49	94.74	70	94.74	95.25	93.87
fault 14	100	99.88	81.73	100	93.76	54.45	90.74	91.99	97	100	99.63	100
fault 16	12.88	23.25	32.54	20.53					27	25.41	28.75	49.69
fault 17	89.38	88.88	72.59	85.61					83	86.61	95.63	96.12
fault 18	89.75	89.5	89.11	89.36					73	89.49	98.88	90.24
fault 19	2.88	3	0.75	1.88					64	22.28	8.38	80.48
fault 20	37.88	45.5	38.17	41.68					71	43.68	48.63	70.59
fault 21	42.75	38.25	34.79	38.17					50	42.68		59.95
average	70.08	71.78	66.36	68.87					75.56	73.42		83.71

https://doi.org/10.1021/acsomega.1c06033
ACS Omega 2022, 7, 2996−3006

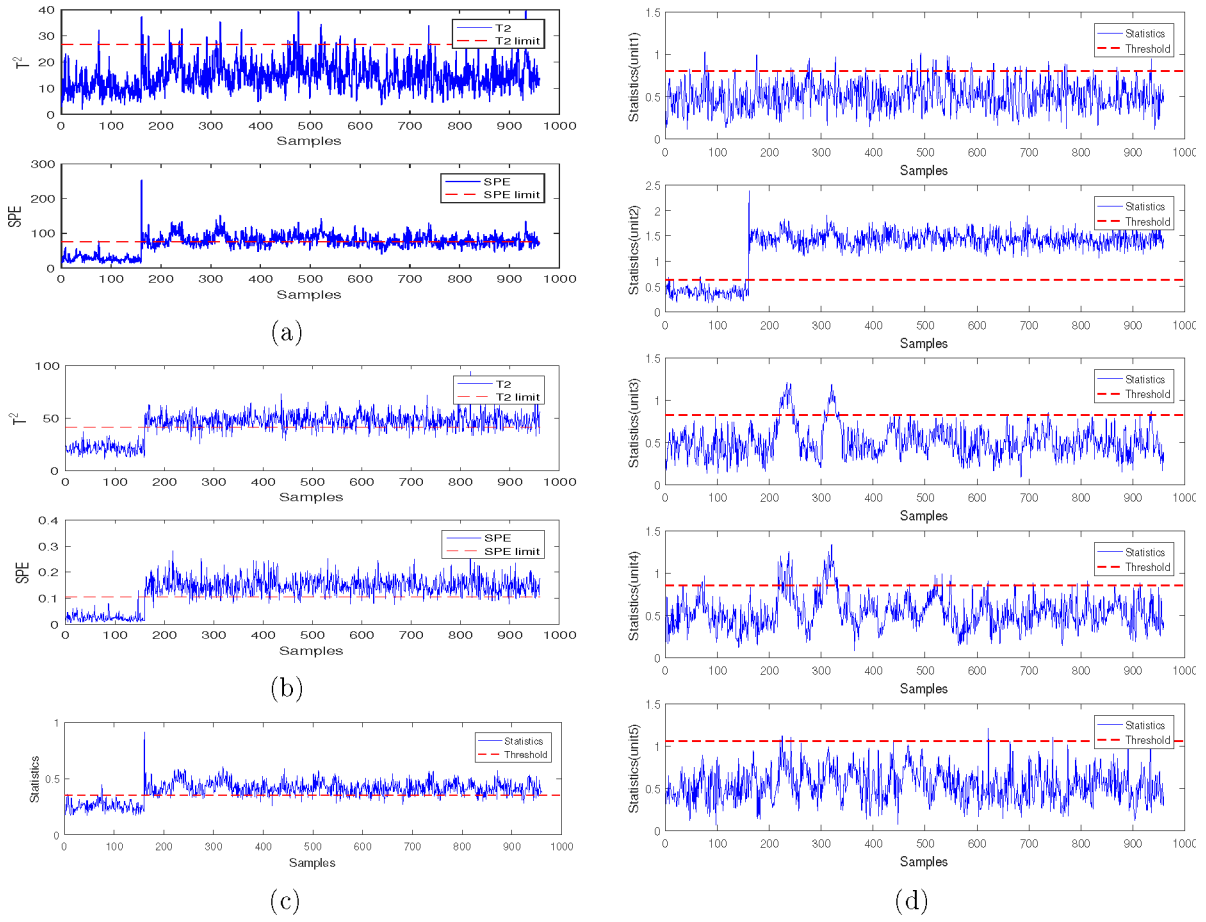

Figure 8. Detection charts of fault 4 in the TE process: (a) GLPP, (b) KPCA, (c) VAE, and (d) DVAE (unit 1 to unit 5).

faults 4, 7, 10, 11, 14, 17, 19, and 20 are significantly higher in one unit compared with others. That is, these faults are more likely to occur in units with higher detection rates. For example, fault 4 is a local fault influencing reactor under cooling water inlet temperature, leading to a step change in measurement of reactor cooling water flow. In addition, the result shows that the FDR of unit 2 is considerably higher than the other four, which agrees with the fault setting. Variables interact with each other throughout the entire process, and the FDRs of some faults are not significantly different in various units. However, DVAE does not lead to poor experimental performance because each unit considers information from local and neighboring units.

For an in-depth discussion, some types of common methods are used for comparison with the proposed distributed VAE. Given that the majority of them are nonlinear approaches that may lead to high FAR, the confidence limitation is set to 99% to ensure a reasonable range of FAR. The FDRs of all five units are shown in Table 5. The detection performance of DVAE is superior to the other methods overall, and the FDRs with faults 1, 6, 7, and 14 are nearly 100%. Note that the performance of fault 5 is unsatisfactory because, through the negative feedback of the system, most of the relevant variables of fault 5 will return to the previous state. In the following section, three types of fault detection charts using KPCA, GLPP, VAE, and DVAE are shown: step fault (fault 4), random fault (fault 11), and unknown fault (fault 19).

Fault 4 is a local fault and caused by step variations in the reactor cooling water (RCW) inlet temperature. The detection results derived via KPCA, GLPP, VAE, and DVAE are presented in Figure 8. In GLPP and KPCA, T^2 and SPE statistics are used to represent the change of principal component space and residual space, respectively. For VAE and DVAE, ED statistics is used to integrate the variations of principal component space and residual space. The detection performance of GLPP is worse than the others, especially for T^2 statistics (Figure 8a). The possible reason is that GLPP is completely linear, which is not suited for the nonlinear process. KPCA (Figure 8b) and VAE (Figure 8c) can detect the fault but fail to detect the fault type. By contrast, the proposed method is able to locate the unit where the fault occurred. Figure 8d shows the results of all five units from top to bottom. The results demonstrate that only unit 2 (reactor) detects the fault without delay (at the 161st sample), while others are not affected by the fault, which is consistent with the fault setting.

Fault 11 is a random variation caused by the inlet temperature changes of RCW, the detection results of which are shown in Figure 9. Overall, the detection performance of DVAE is superior over GLPP, KPCA, and VAE. In particular, although GLPP (Figure 9a) and KPCA (Figure 9b) can relatively detect fault 11, the statistics fluctuate significantly. VAE (Figure 9c) and DVAE (Figure 9d) achieved good detection results for fault 11, whereas DVAE has a higher detection rate, reaching 90.11%. Moreover, the statistics of unit 2 is evidently different from the other four units (Figure 9d). Fault 19 is an unknown fault. The detection results are shown in Figure 10. Evidently, only DVAE shows good detection performance of fault 19, while GLPP, KPCA, and VAE cannot

https://doi.org/10.1021/acsomega.1c06033
ACS Omega 2022, 7, 2996−3006

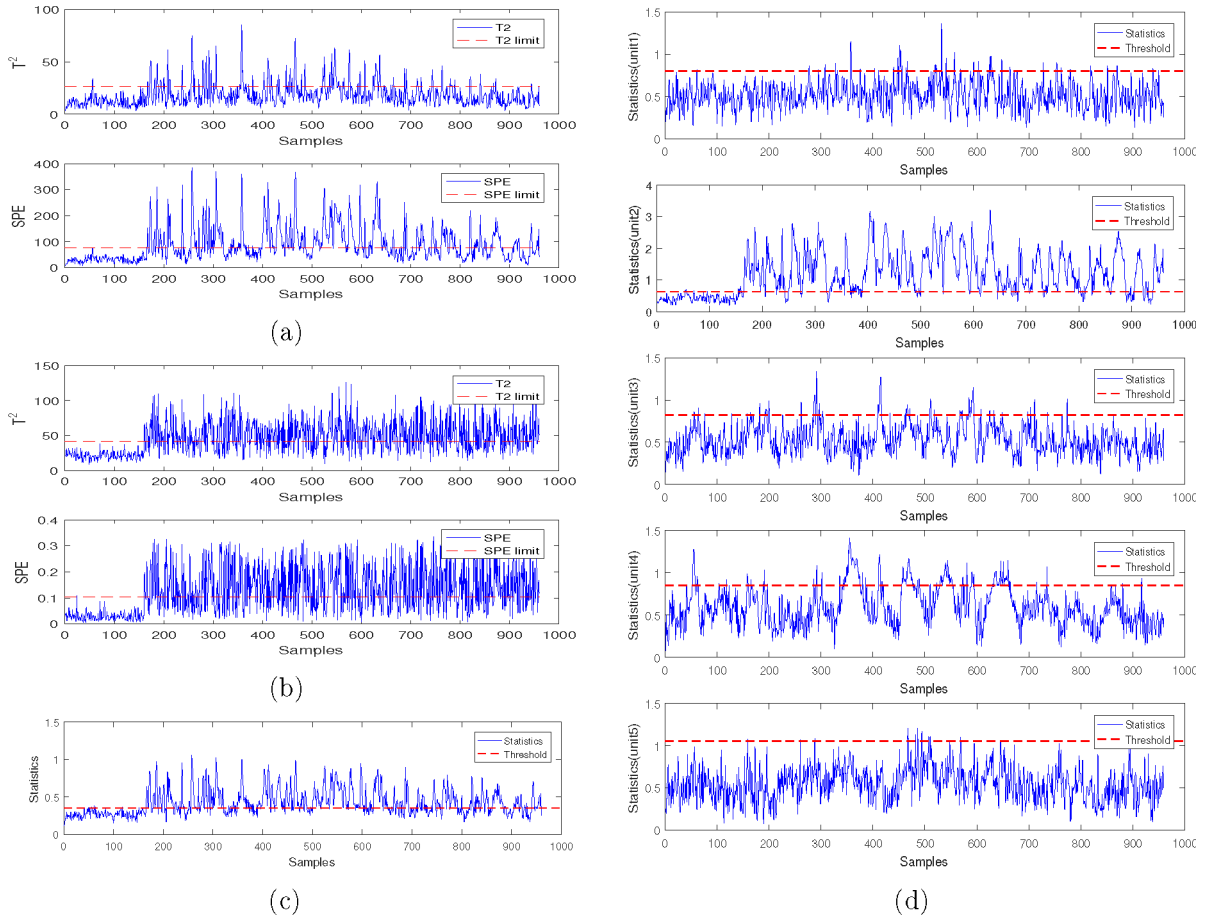

Figure 9. Detection charts of fault 11 in the TE process: (a) GLPP, (b) KPCA, (c) VAE, and (d) DVAE (unit 1 to unit 5).

alarm the fault immediately. Thus, by comparing several methods, a higher fault detection sensitivity and the capability of the fault location of DVAE is again demonstrated.

Fault Detection with Missing Data. Missing data are among the problems that are frequently encountered in data analysis. In this study, we construct 5−30% random missing data to simulate the normal operating data to explain the influence of missing data on detection performance. For comparative analysis, the following strategies are adopted to address missing values: (1) Replace the missing data with the data reconstructed by DVAE. (2) Fill in the missing data with the sample mean.

The average FDR error is used to evaluate the detection performance of missing data, which is calculated as follows: $\mathrm{Err} = \sum_{i=1}^{J} (D_i - \hat{D}_i)/J$, where J is the number of effective faults and D and $\hat{D}$ denote the FDR of complete data and missing data, respectively. The decline in the detection results is shown in Figure 11 by using unit 5 as an example. As the proportion of missing data increases, the FDR of the mean filling strategy rapidly decreases. By contrast, the performance of DVAE in reconstruction has not significantly changed compared with that when the data are complete. The data can be completely reconstructed when only a few values are missing. This result shows that reconstruction with DVAE provides an excellent outcome. Therefore, the proposed DVAE method has a good effect on the reconstruction of missing data.

CONCLUSION

This study proposes a novel distributed fault detection approach based on DVAE. This approach is suitable for large-scale multiunit fault detection problems. First, the entire industrial process is divided into components by mechanism. Second, local and neighboring unit data sets are used to train the DVAE model. Given this improvement, the proposed method can determine the correlation between local unit data and latent variables and also describe the neighboring unit data and latent variables. The results for the case study show that the proposed fault detection approach outperforms the existing latent-variable-based methods in nonlinear and non-normal situations in high-dimensional processes. In addition, it has been verified to be capable of locating the local fault. Given the characteristics of the generation model, it also shows good performance in missing data processing.

The proposed DVAE distributed fault detection model is highly suitable for large-scale processes. The model considers the variable relationship with the surrounding neighboring units and can determine the approximate scope of local faults. However, this study focuses on a single-mode process, and fault detection performance relies heavily on data-based models. Therefore, future studies should focus on the extension of the model to multimodal processes and the incorporation of process knowledge into the proposed method.

https://doi.org/10.1021/acsomega.1c06033
ACS Omega 2022, 7, 2996−3006

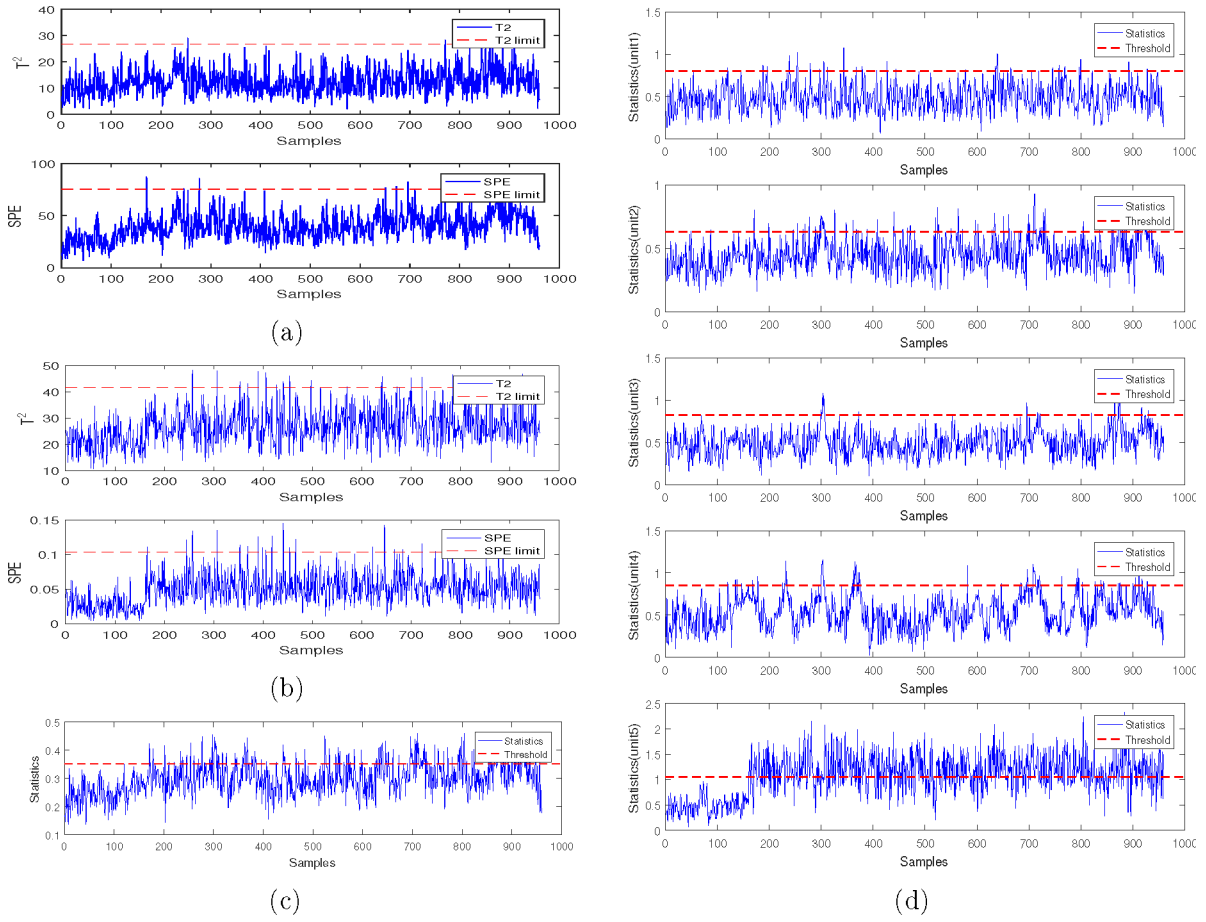

Figure 10. Detection charts of fault 19 in the TE process: (a) GLPP, (b) KPCA, (c) VAE, and (d) DVAE (unit 1 to unit 5).

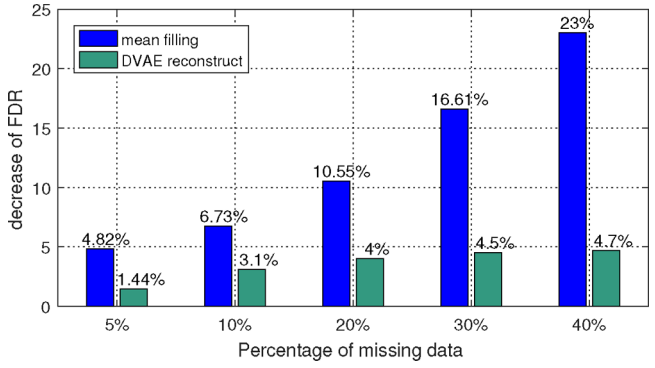

Figure 11. Variation of FDR with missing data in unit 5.

AUTHOR INFORMATION

Corresponding Author

Yi Chai − *College of Automation, Chongqing University, Chongqing 400044, China; State Key Laboratory of Power Transmission Equipment and System Security and New Technology, Chongqing University, Chongqing 400044, China*; Email: Chaiyi@cqu.edu.cn

Authors

Chenghong Huang − *College of Automation, Chongqing University, Chongqing 400044, China; State Key Laboratory of Power Transmission Equipment and System Security and New Technology, Chongqing University, Chongqing 400044, China*; orcid.org/0000-0002-6252-653X

Zheren Zhu − *College of Control Science and Engineering, Zhejiang University, Hangzhou 310058, China*

Bowen Liu − *College of Automation, Chongqing University, Chongqing 400044, China; State Key Laboratory of Power Transmission Equipment and System Security and New Technology, Chongqing University, Chongqing 400044, China*

Qiu Tang − *College of Control Science and Engineering, Shandong University, Shandong 250061, China*

Complete contact information is available at: https://pubs.acs.org/10.1021/acsomega.1c06033

Notes

The authors declare no competing financial interest.

ACKNOWLEDGMENTS

This work is supported by the National Key Research and Development Project (2019YFB2006603) and the National Natural Science Foundation of China (61633005, U2034209).

REFERENCES

(1) Ge, Z. Review on data-driven modeling and monitoring for plant-wide industrial processes. *Chemom. Intell. Lab. Syst.* **2017**, *171*, 16−25.

(2) Yin, S.; Li, X.; Gao, H.; Kaynak, O. Data-Based Techniques Focused on Modern Industry: An Overview. *IEEE Trans. Ind. Electron.* **2015**, *62*, 657−667.

(3) Ma, L.; Dong, J.; Peng, K. A Novel Hierarchical Detection and Isolation Framework for Quality-Related Multiple Faults in Large-Scale Processes. *IEEE Trans. Ind. Electron.* **2020**, *67*, 1316−1327.
(4) Yin, S.; Ding, S. X.; Haghani, A.; Hao, H.; Zhang, P. A comparison study of basic data-driven fault diagnosis and process monitoring methods on the benchmark Tennessee Eastman process. *J. Process Control* **2012**, *22*, 1567−1581.
(5) Alauddin, M.; Khan, F.; Imtiaz, S.; Ahmed, S. A Bibliometric Review and Analysis of Data-Driven Fault Detection and Diagnosis Methods for Process Systems. *Ind. Eng. Chem. Res.* **2018**, *57*, 10719−10735.
(6) Tao, Y.; Shi, H.; Song, B.; Tan, S. Parallel quality-related dynamic principal component regression method for chemical process monitoring. *J. Process Control* **2019**, *73*, 33−45.
(7) Nomikos, P.; MacGregor, J. F. Monitoring batch processes using multiway principal component analysis. *AIChE J.* **1994**, *40*, 1361−1375.
(8) Jia, Z.; Zeng, Y.; Zhang, Y.; Liang, W. Local class-specific discriminant analysis with variable weighting and its application in fault diagnosis. *Comput. Chem. Eng.* **2020**, *141*, 107023.
(9) He, X.; Niyogi, P. Locality Preserving Projections. Proceedings of the 16th International Conference on Neural Information Processing Systems. 2003, pp 153−160.
(10) Lee, J.-M.; Yoo, C.; Lee, I.-B. Statistical process monitoring with independent component analysis. *J. Process Control* **2004**, *14*, 467−485.
(11) Tao, Y.; Shi, H.; Song, B.; Tan, S. A Novel Dynamic Weight Principal Component Analysis Method and Hierarchical Monitoring Strategy for Process Fault Detection and Diagnosis. *IEEE Trans. Ind. Electron.* **2020**, *67*, 7994−8004.
(12) Tang, Q.; Chai, Y.; Qu, J.; Fang, X. Industrial process monitoring based on Fisher discriminant global-local preserving projection. *J. Process Control* **2019**, *81*, 76−86.
(13) Lee, J.-M.; Yoo, C.; Choi, S. W.; Vanrolleghem, P. A.; Lee, I.-B. Nonlinear process monitoring using kernel principal component analysis. *Chem. Eng. Sci.* **2004**, *59*, 223−234.
(14) Yang, M.-H. Kernel Eigenfaces vs. Kernel Fisherfaces: Face Recognition Using Kernel Methods. *Proceedings of the Fifth IEEE International Conference on Automatic Face and Gesture Recognition. USA,* **2002**, 215.
(15) Yu, H.; Khan, F. Improved latent variable models for nonlinear and dynamic process monitoring. *Chem. Eng. Sci.* **2017**, *168*, 325−338.
(16) Yu, H.; Khan, F.; Garaniya, V.; Ahmad, A. Self-Organizing Map Based Fault Diagnosis Technique for Non-Gaussian Processes. *Ind. Eng. Chem. Res.* **2014**, *53*, 8831−8843.
(17) Liu, B.; Chai, Y.; Liu, Y.; Huang, C.; Wang, Y.; Tang, Q. Industrial process fault detection based on deep highly-sensitive feature capture. *J. Process Control* **2021**, *102*, 54−65.
(18) Yu, H.; Khan, F.; Garaniya, V. Nonlinear Gaussian Belief Network based fault diagnosis for industrial processes. *J. Process Control* **2015**, *35*, 178−200.
(19) Arunthavanathan, R.; Khan, F.; Ahmed, S.; Imtiaz, S.; Rusli, R. Fault detection and diagnosis in process system using artificial intelligence-based cognitive technique. *Comput. Chem. Eng.* **2020**, *134*, 106697.
(20) Amin, M. T.; Imtiaz, S.; Khan, F. Process system fault detection and diagnosis using a hybrid technique. *Chem. Eng. Sci.* **2018**, *189*, 191−211.
(21) Yan, S.; Yan, X. Quality-Driven Autoencoder for Nonlinear Quality-Related and Process-Related Fault Detection Based on Least-Squares Regularization and Enhanced Statistics. *Ind. Eng. Chem. Res.* **2020**, *59*, 12136−12143.
(22) Jiang, L.; Ge, Z.; Song, Z. Semi-supervised fault classification based on dynamic Sparse Stacked auto-encoders model. *Chemom. Intell. Lab. Syst.* **2017**, *168*, 72−83.
(23) Kingma, D. P.; Welling, M. Auto-Encoding Variational Bayes, 2014.
(24) He, Y.-L.; Ma, Y.; Xu, Y.; Zhu, Q.-X. Fault Diagnosis Using Novel Class-Specific Distributed Monitoring Weighted Naive Bayes: Applications to Process Industry. *Ind. Eng. Chem. Res.* **2020**, *59*, 9593−9603.
(25) Ma, L.; Dong, J.; Peng, K. A Novel Hierarchical Detection and Isolation Framework for Quality-Related Multiple Faults in Large-Scale Processes. *IEEE Trans. Ind. Electron.* **2020**, *67*, 1316−1327.
(26) Jiang, Q.; Huang, B.; Ding, S. X.; Yan, X. Bayesian Fault Diagnosis With Asynchronous Measurements and Its Application in Networked Distributed Monitoring. *IEEE Trans. Ind. Electron.* **2016**, *63*, 6316−6324.
(27) He, Y.-L.; Zhao, Y.; Zhu, Q.-X.; Xu, Y. Online Distributed Process Monitoring and Alarm Analysis Using Novel Canonical Variate Analysis with Multicorrelation Blocks and Enhanced Contribution Plot. *Ind. Eng. Chem. Res.* **2020**, *59*, 20045−20057.
(28) Xu, X.; Ding, J. Decentralized dynamic process monitoring based on manifold regularized slow feature analysis. *J. Process Control* **2021**, *98*, 79−91.
(29) Cao, Y.; Chen, Z.; Yuan, X.; Wang, Y.; Gui, W. Distributed PCA for plant-wide processes monitoring with partial block communication. *Control and Decision* **2020**, *35*, 1281−1290.
(30) Jiang, J.; Jiang, Q. Variational Bayesian probabilistic modeling framework for data-driven distributed process monitoring. *Control Engineering Practice* **2021**, *110*, 104778.
(31) Jiang, Q.; Yan, S.; Cheng, H.; Yan, X. Local-Global Modeling and Distributed Computing Framework for Nonlinear Plant-Wide Process Monitoring With Industrial Big Data. *IEEE Transactions on Neural Networks and Learning Systems* **2021**, *32*, 3355−3365.
(32) Chiang, L.; Russell, E.; Braatz, R. *Fault Detection and Diagnosis in Industrial Systems*; Springer-Verlag: London, 2001.
(33) Downs, J.; Vogel, E. A plant-wide industrial process control problem. *Comput. Chem. Eng.* **1993**, *17*, 245−255.
(34) Huang, C.; Chai, Y.; Liu, B.; Tang, Q.; Qi, F. Industrial process fault detection based on KGLPP model with Cam weighted distance. *J. Process Control* **2021**, *106*, 110−121.
(35) Russell, E. L.; Chiang, L. H.; Braatz, R. D. Fault detection in industrial processes using canonical variate analysis and dynamic principal component analysis. *Chemom. Intell. Lab. Syst.* **2000**, *51*, 81−93.
(36) Grbovic, M.; Li, W.; Xu, P.; Usadi, A. K.; Song, L.; Vucetic, S. Decentralized fault detection and diagnosis via sparse PCA based decomposition and Maximum Entropy decision fusion. *J. Process Control* **2012**, *22*, 738−750.
(37) Maas, A. L. Rectifier Nonlinearities Improve Neural Network Acoustic Models, 2013.
(38) Lee, S.; Kwak, M.; Tsui, K.-L.; Kim, S. B. Process monitoring using variational autoencoder for high-dimensional nonlinear processes. *Engineering Applications of Artificial Intelligence* **2019**, *83*, 13−27.
(39) Yu, H.; Khan, F.; Garaniya, V. An Alternative Formulation of PCA for Process Monitoring Using Distance Correlation. *Ind. Eng. Chem. Res.* **2016**, *55*, 656−669.

https://doi.org/10.1021/acsomega.1c06033
ACS Omega 2022, 7, 2996−3006